BIOLOGICAL SCIENCES: Developmental Biology

Polycomb suppresses a female gene regulatory network in Sertoli cells.

So Maezawa[a, b, c, d*], Masashi Yukawa[b, e], Kazuteru Hasegawa[a, b], Ryo Sugiyama[c], Mengwen Hu[a, b, f], Miguel Vidal[g], Haruhiko Koseki[h], Artem Barski[b, e], Tony DeFalco[a, b], and Satoshi H. Namekawa[a, b, f*]

[a] Division of Reproductive Sciences, Division of Developmental Biology, Perinatal Institute, Cincinnati Children's Hospital Medical Center, Cincinnati, Ohio, 45229, USA

[b] Department of Pediatrics, University of Cincinnati College of Medicine, Cincinnati, Ohio, 45229, USA

[c] Department of Animal Science and Biotechnology, School of Veterinary Medicine, Azabu University, Sagamihara, Kanagawa 252-5201, Japan

[d] Faculty of Science and Technology, Department of Applied Biological Science, Tokyo University of Science, Chiba 278-8510, Japan.

[e] Division of Allergy and Immunology, Division of Human Genetics, Cincinnati Children's Hospital Medical Center, Cincinnati, Ohio, 45229, USA

[f] Department of Microbiology and Molecular Genetics, University of California, Davis, California, 95616, USA

[g] Centro de Investigaciones Biológicas Margarita Salas, Department of Cellular and Molecular Biology, Madrid 28040, Spain

[h] Developmental Genetics Laboratory, RIKEN Center for Allergy and Immunology, Yokohama, Kanagawa, Japan

*Corresponding authors: E-mail: s-maezawa@rs.tus.ac.jp; snamekawa@ucdavis.edu

Keywords: Polycomb, Sertoli cells, Sex determination, Testis, Spermatogenesis

Abstract

Gonadal sex determination is controlled by the support cells of testes and ovaries. Sexual fate becomes labile and interchangeable with the removal of specific, critical transcription factors from postnatal gonad support cells. In Sertoli cells, the specific support cells for postnatal testes, the epigenetic mechanism that maintains cellular memory to suppress female sexual differentiation remains unknown. Here, we show that, in postnatal Sertoli cells, Polycomb suppresses a female gene regulatory network. Through genetic ablation, we removed Polycomb repressive complex 1 (PRC1) from embryonic Sertoli cells after sex determination. PRC1-depleted postnatal Sertoli cells exhibited defective proliferation and cell death, leading to the degeneration of adult testes. In adult Sertoli cells, PRC1 suppressed the specific, critical genes required for granulosa cells, the support cells of ovaries, thereby inactivating the female gene regulatory network. The underlying chromatin of female genes was coated with Polycomb-mediated repressive modifications: PRC1-mediated H2AK119ub and PRC2-mediated H3K27me3. Taken together, we identify a critical mechanism centered on Polycomb that maintains the male fate in adult testes.

Significance

Sex differences in mammals are defined by the reproductive organs, testes and ovaries. In testes and ovaries, sexual fate is determined by Sertoli cells and granulosa cells, respectively, which are supporting cells derived from common somatic progenitors. Critical transcription factors determine sexual fate of Sertoli and granulosa cells, and, remarkably, removal of these factors reverses sexual identity. Therefore, sexual fate is surprisingly plastic. Here we address a long-standing question in developmental biology of how male sexual fate is maintained in testes throughout life. We show that epigenetic machinery of Polycomb repressive complex 1 (PRC1) suppresses a female gene regulatory network in Sertoli cells. Thus, Polycomb preserves cellular memory and sexual identity of Sertoli cells, thereby defining the testicular fate.

Introduction

In mammals, gonadal sex determination takes place in the bipotential somatic cell precursors of male Sertoli cells and female granulosa cells in embryos (1-3). Sertoli cells are the first somatic cells to differentiate in the XY gonad. In testes, Sertoli cells function as a regulatory hub for both differentiation and survival of germ cells, thereby determining male sexual fate (4). The mechanisms maintaining the male cellular identity of Sertoli cells are fundamental for adult testicular functions, including spermatogenesis and hormone production.

At the time of sex determination in embryos, the commitment to the male fate is triggered by the expression of the Y-linked *Sry* gene, and, subsequently, the female fate is suppressed (1-3). Distinct gene regulatory networks promote the male or female fate and are regulated by strong feedback loops that antagonize each other, canalizing one fate from the other (3). Sexual fate is interchangeable even after the initial commitment to Sertoli cells or granulosa cells with the removal of specific, critical transcription factors. The loss of *Dmrt1* in Sertoli cells leads to derepression of *Foxl2*, a master regulator of granulosa cell fate, and transdifferentiation of cell fate from Sertoli to granulosa cells (5, 6). On the other hand, the loss of *Foxl2* in granulosa cells leads to derepression of the male gene network and transdifferentiation of cell fate from granulosa to Sertoli cells (7). These findings, together with follow-up studies (8-12), suggest that active repression of the alternate sexual fate is important for both testicular and ovarian function, even in adult life.

Epigenetic silencing mechanisms serve as molecular switches for the sex determination of bipotential somatic cell precursors. The deletion of a Polycomb gene *Cbx2* results in male to female reversal (13), which is mediated through suppression of genes required for the female fate (14). Additionally, regulation of H3K9 methylation is important for the male sexual fate (15). Although these studies highlight the importance of epigenetic mechanisms for initial sex determination, the epigenetic mechanisms by which male cellular identity is maintained through cell divisions and the proliferation of Sertoli cells remain to be determined.

Polycomb proteins suppress non-lineage-specific genes and define cellular identities of each lineage in stem cells and in development (16-18). In this study, we show that Polycomb suppresses the female gene regulatory network in postnatal Sertoli cells, thereby promoting the male gene regulatory network to ensure male cell fate. We generated loss-of-function mouse models of Polycomb repressive complex 1 (PRC1) in Sertoli cells after initial sex determination.

94 We show that PRC1 is required for the proliferation of Sertoli cells, as well as the suppression of
95 non-lineage-specific genes and the female gene regulatory network in Sertoli cells. Taken together,
96 we identify a critical mechanism centered on Polycomb that maintains male fate in adult testes.
97
98 **Results**
99 **PRC1 in Sertoli cells is required for the maintenance of spermatogenesis.** In postnatal Sertoli
100 cells (which are detected by the Sertoli cell marker GATA4), RNF2 is highly expressed and the
101 RNF2-mediated epigenetic mark H2AK119ub is abundant (Fig.1*A*), which suggests PRC1
102 functions in these cells. To determine the function of PRC1, we generated a PRC1 loss-of-function
103 mouse model by removing two redundant catalytic subunits, RNF2 and RING1 (19). We generated
104 a conditional deletion of *Rnf2* (*Rnf2*cKO) using *Amh*-Cre, which is expressed specifically in Sertoli
105 cells after embryonic day 14.5 (E14.5) (20), in a background of *Ring1*-knockout (KO) mice (*Amh*-
106 Cre; *Rnf2*cKO; *Ring1*-KO: termed PRC1$^{Amh\text{-}Cre}$cKO: PRC1AcKO). Although RNF2 appears to be
107 the most active component in the heterodimeric E3 ligases of PRC1, the RNF2 paralog RING1 can
108 partially compensate for the loss of RNF2 (19). Therefore, we made a conditional deletion of *Rnf2*
109 in a background of *Ring1*-KO mice, which are viable and do not have fertility defects (21). This
110 strategy enabled us to define the function of RNF2 without compensation from RING1, while also
111 representing a "complete" loss-of-function of PRC1 as shown in testicular germ cells (22) and in
112 other biological contexts (19, 23, 24). Since PRC1 has various components, including CBX2 (25),
113 this strategy allows us to determine the global function of PRC1. At the same time, the use of *Amh*-
114 Cre allowed us to test the function of PRC1, specifically after the completion of sex determination
115 at E12.5.
116
117 PRC1AcKO males have smaller testes compared with littermate controls that harbored
118 floxed alleles for *Rnf2* on a *Ring1*-KO background without *Amh*-Cre (termed PRC1 control:
119 PRC1ctrl: Fig. 1*B* and *C*). We confirmed efficient *Amh*-Cre-mediated recombination by observing
120 depletion of the RNF2-mediated mark, H2AK119ub, in GATA4^{+} Sertoli cells of PRC1AcKO testes
121 at E15.5 (> 95 % efficiency: Fig. 1*D*) and at postnatal day 7 (P7: Fig. 1*E*). In 6 week-old
122 PRC1AcKO testes, while the tubules with H2AK119ub^{+} Sertoli cells (escaped Cre-mediated
123 deletion) appear to have normal morphology, we frequently observed disorganization of testicular
124 tubules that contain H2AK119ub^{-} Sertoli cells (underwent Cre-mediated deletion: arrowheads, Fig.
125 S1), suggesting a critical function of PRC1 in Sertoli cells in the organization of testicular tubules.
126 This mosaic pattern is presumably due to incomplete Cre-mediated recombination, as the Sertoli
127 cells that escaped Cre-mediated recombination might have repopulated the testes. Consistent with

128 this interpretation, PRC1AcKO males are subfertile, and 9 out of 15 wild-type females mated with
129 8-11-week old PRC1AcKO males gave birth (Fig. 1*F*) at comparable litter sizes (Fig.1*G*).
130 Interestingly, fecundity decreased in aged PRC1AcKO males (5 months old), as litter sizes were
131 smaller as compared to controls (Fig. 1*G*). To further examine the phenotype, we measured the
132 blood levels of three hormones critical for testicular homeostasis: although the levels of testosterone
133 and estradiol were comparable between cKO and control mice, follicle-stimulating hormone was
134 increased in mutants (Fig. 1*H*). As follicle stimulating hormone levels are regulated by a feedback
135 mechanism involving Sertoli cells (26), we infer that the dysfunction of Sertoli cells and testicular
136 degeneration caused increased follicle stimulating hormone levels to recover Sertoli cell function.
137
138 To determine the cause of testicular degeneration, we next examined the proliferation of
139 Sertoli cells. In normal mouse development, Sertoli cells proliferate in fetal and neonatal testes
140 until approximately 2 weeks after birth, and the number of Sertoli cells in adult testes determines
141 both testis size and daily sperm production (27). In P7 control testes, GATA4^{+} Sertoli cells
142 occasionally co-expressed an S phase marker, PCNA, and another marker of active cell cycle, Ki67
143 (Fig. 2*A*), consistent with the active proliferation of Sertoli cells. However, in PRC1AcKO testes,
144 GATA4^{+} Sertoli cells were largely devoid of PCNA and Ki67 (Fig. 2*A*), suggesting impaired
145 proliferation of PRC1AcKO Sertoli cells. Next, we independently confirmed the proliferation
146 phenotype by using EdU labeling of actively proliferating cells. EdU was abdominally
147 administrated to P7 mice, and testicular sections were examined the following day. While GATA4^{+}
148 Sertoli cells were occasionally EdU^{+} (approximately one-fouth) in control testes , GATA4^{+} Sertoli
149 cells were devoid of EdU signal in PRC1AcKO testes (Fig. 2*B*). Additional labeling of H2AK119ub
150 confirmed the loss of PRC1 function in GATA4^{+} Sertoli cells from PRC1AcKO testes (Fig. 2*B*).
151 From these results, we conclude that the loss of PRC1 disrupts the proliferation of Sertoli cells.
152 This is in contrast with PRC1's function in testicular germ cells, in which the loss of PRC1 does
153 not affect proliferation but instead causes apoptotic cell death (22). This difference suggests a
154 unique function of PRC1 in Sertoli cells that is distinct from its function in germ cells.
155
156 **In Sertoli cells, PRC1 suppresses genes required for granulosa cells.** We next sought to
157 determine the genes regulated by PRC1 in Sertoli cells. In PRC1AcKO testes, some Sertoli cells
158 escaped *Amh*-Cre-mediated recombination. Thus, it was difficult to specifically isolate Sertoli cells
159 that underwent PRC1 depletion. To precisely determine the function of PRC1 in gene regulation in
160 Sertoli cells, we used an alternative strategy: we isolated Sertoli cells from a mouse line in which
161 conditional deletion of PRC1 can be induced by tamoxifen-inducible Cre-mediated recombination

162 under the control of the endogenous ROSA26 promoter (*ROSA26*-Cre^{ERT}; *Rnf2*$^{floxed/floxed}$; *Ring1*-
163 KO: termed PRC1$^{ROSA26\text{-}CreERT}$cKO: PRC1RcKO). After isolating Sertoli cells from P7 testes, we
164 cultured Sertoli cells for 4 days in the presence of 4-hydroxytamoxifen (4-OHT), and performed
165 RNA-sequencing (RNA-seq: Fig.3*A*). As a control, we isolated Sertoli cells from control mice
166 (*Rnf2*$^{floxed/floxed}$; *Ring1*-KO) and cultured them in the same 4-OHT conditions. We performed RNA-
167 seq for two independent biological replicates and confirmed reproducibility between biological
168 replicates (Fig. S1*A*).
169
170 Our RNA-seq analyses demonstrated that 338 genes were upregulated in PRC1RcKO
171 Sertoli cells as compared to controls, while 307 genes were downregulated in PRC1RcKO Sertoli
172 cells (Fig. 3*A* and *B*). Gene ontology (GO) analysis showed that upregulated genes were enriched
173 for functions in neural differentiation, skeletal system, and cell adhesion (Fig. 3*D*). These categories
174 suggest that PRC1 suppressed expression of non-lineage-specific genes in Sertoli cells. On the
175 other hand, GO analysis revealed that downregulated genes were enriched for functions in the cell
176 cycle and M phase (Fig. 3*D*). This result is in accord with the cell cycle arrest we found in
177 PRC1AcKO Sertoli cells (Fig. 2).
178
179 Since we anticipated suppression of genes required for granulosa cells by PRC1 in Sertoli
180 cells, we next investigated the expression level of key genes required for granulosa cells. In
181 PRC1RcKO Sertoli cells, genes required for female sexual development were upregulated: these
182 genes included *Rspo1,* an activator of the Wnt pathway (29), and *Foxl2,* a key transcription factor
183 for granulosa cells (30) (Fig. 3*E*). Importantly, these female genes suppress the male fate, and the
184 loss of these genes leads to female-to-male sex reversal (30-32). Consistent with the antagonistic
185 function of these female genes with the male pathway, key sex determination genes for the male
186 pathway were downregulated in PRC1RcKO Sertoli cells: these genes included *Sox9,* an
187 evolutionarily conserved gene for sex determination, which directs the male pathway downstream
188 of *Sry* (33), and *Dmrt1* (34, 35), male-determining signalling (Fig. 3*E*).
189
190 To determine whether the suppression of female genes was directly regulated by PRC1, we
191 performed chromatin immunoprecipitation sequencing (ChIP-seq) of PRC1-mediated H2AK119ub
192 in isolated wild-type Sertoli cells. We further performed ChIP-seq of H3K27me3 in Sertoli cells
193 since PRC2-mediated H3K27me3 is regulated by PRC1 and its mediated mark H2A119ub (37, 38).
194 We performed ChIP-seq for two independent biological replicates and confirmed the
195 reproducibility between biological replicates (Fig. S1*B*). We confirmed the enrichment of

196 H2AK119ub and H3K27me3 around transcription start sites (TSSs) of *Rspo1* and *Foxl2* (Fig. 3*F*).
197 Compared to the enrichment of H2AK119ub on these female genes, enrichment of H2AK119ub
198 was relatively low on the TSSs of the male genes, *Sox9* and *Dmrt1*. Therefore, we conclude that
199 PRC1 directly binds and suppresses *Rspo1* and *Foxl2*.
200
201 Track views of these ChIP-seq data show that all three marks were enriched at *Foxl2* and
202 *Rspo1* loci (Fig. 4*A*). Furthermore, enrichment of these three marks was found in other loci such as
203 *Foxf2*, the mutation of which appears in patients with disorders of sex development (39), and
204 *Hoxd13*, which is involved in female reproductive tract development (40). These results suggest
205 that PRC1 works with PRC2 to suppress female genes as well as developmental regulators such as
206 *Fox* and *Hox* genes, which are the classical targets of Polycomb-mediated gene repression (41).
207
208 To determine the features of genome-wide gene repression mediated by Polycomb
209 complexes, we analyzed the enrichment of H2AK119ub, H3K27me3, and RNF2 on the upregulated
210 genes in PRC1RcKO Sertoli cells. H2AK119ub, H3K27me3, and RNF2 were all significantly
211 enriched on the TSSs of upregulated genes in PRC1RcKO Sertoli cells as compared to all genes in
212 the genome (Fig. 4*B*). Additional enrichment analysis confirmed the co-enrichment of H2AK119ub
213 and H3K27me3 (Fig. 4*C,* upper panels) as well as co-enrichment of H2AK119ub and RNF2 (Fig.
214 4*C,* lower panels) on upregulated genes in PRC1RcKO Sertoli cells. Furthermore, average tag
215 density analysis confirmed that enrichment of H2AK119ub on upregulated genes in PRC1RcKO
216 Sertoli cells occured on upstream regions, gene bodies, and downstream regions with the highest
217 enrichment near TSSs (Fig. 4*D*). We found a similar distribution of H3K27me3 around the gene
218 bodies of upregulated genes in PRC1RcKO Sertoli cells (Fig. S2). Together, these results
219 confirmed the genome-wide, global functions of PRC1 in the direct regulation of gene repression
220 in Sertoli cells.
221
222 **Polycomb globally inactivates the female gene regulatory network in postnatal Sertoli cells.**
223 Previous studies have suggested that sex determination is canalized by the interconnected,
224 antagonistic network of genes both in males and in females that are controlled by feedback
225 mechanisms (3). Since Polycomb is implicated in the maintenance of sex-specific gene regulatory
226 networks through the PRC2-mediated mark H3K27me3 (14), we hypothesized that PRC1 globally
227 inactivates the female gene regulatory network in postnatal Sertoli cells. Since male- and female-
228 specific gene networks are regulated immediately after sex determination during fetal stages (42),
229 we reasoned that female gene network suppression in fetal Sertoli cells is maintained by PRC1 in

230 postnatal Sertoli cells. To test this hypothesis, we examined the expression profiles of specifically
231 expressed genes in E13.5 granulosa cells (42) (Fig. S3), termed “pre-granulosa genes” in postnatal
232 Sertoli cells. We found that pre-granulosa genes were upregulated in PRC1RcKO postnatal Sertoli
233 cells as compared to other genes (Fig. 5*A*). On the other hand, specifically expressed genes in E13.5
234 Sertoli cells (42) (Fig. S3), termed “pre-Sertoli genes," were downregulated in PRC1RcKO
235 postnatal Sertoli cells as compared to other genes (Fig. 5*A*). We further examined the correlation
236 of each gene and found that pre-granulosa genes were highly correlated with upregulated genes in
237 PRC1RcKO postnatal Sertoli cells, while pre-Sertoli genes were highly correlated with
238 downregulated genes in PRC1RcKO postnatal Sertoli cells (Fig. 5*B*). These results suggest that
239 PRC1 maintains suppression of the female gene regulatory network, which is initiated at the time
240 of sex determination and is maintained throughout the development of postnatal Sertoli cells.
241
242 We next sought to determine whether PRC1 directly suppresses the female gene regulatory
243 network in postnatal Sertoli cells. H2AK119ub is significantly enriched on TSSs of pre-granulosa
244 genes compared to other genes and pre-Sertoli genes (Fig. 5*C*). Among pre-granulosa genes,
245 enrichment of H2AK119ub is positively correlated with upregulated genes in PRC1RcKO
246 postnatal Sertoli cells (Fig. 5*D*). We further identified the enrichment of H3K27me3 on TSSs of
247 pre-granulosa genes in postnatal Sertoli cells (Fig. S4*A*), and the correlation between H3K27me3
248 and upregulated genes on the pre-granulosa genes in PRC1RcKO postnatal Sertoli cells (Fig. S4*B*).
249 Together, we conclude that PRC1 globally inactivates the female gene regulatory network in
250 postnatal Sertoli cells.
251
252 **Discussion**
253 In this study, we demonstrated that PRC1 is required for proliferation of Sertoli cells and
254 suppression of the non-lineage-specific gene expression program and the female gene regulatory
255 network. Among these functions, we infer that suppression of the female gene regulatory network
256 is the key mechanism to ensure male fate in addition to canonical functions of PRC1, which controls
257 proliferation and suppression of non-lineage-specific gene expression programs. Although we did
258 not observe complete infertility using *Amh*-Cre, presumably due to the repopulation of Sertoli cells
259 that escaped Cre-mediated recombination, smaller testis size and abnormal tubule organization of
260 cKO testes (Fig. 1) suggest that PRC1 is critical for physiological functions of Sertoli cells. Below,
261 we discuss two molecular aspects underlying these physiological phenotypes: control of
262 proliferation and suppression of the female gene regulatory network.
263

264 The proliferation of Sertoli cells is a critical determinant of testicular functions because the
265 number of Sertoli cells defines testicular functions (27). Rapid proliferation is a prominent feature
266 of juvenile Sertoli cells. In general, Polycomb proteins are associated with the cell cycle checkpoint
267 by directly suppressing the tumor suppressor locus *Cdkn2a*/*Ink4a*/*Arf* (43), which functions as a
268 barrier to cancer transformation (44). Therefore, enhanced Polycomb activity is a frequent feature
269 of human tumors. We found that *Cdkn2a* was derepressed in PRC1RcKO Sertoli cells
270 (approximately 2.5-fold upregulation: PRKM value for PRC1RcKO: 32.1 v.s. PRC1ctrl: 13.0).
271 Therefore, our results suggest that PRC1 promotes the rapid proliferation of Sertoli cells by
272 suppressing *Cdkn2a.* The function of PRC1 in Sertoli cell proliferation is distinct from Polycomb
273 functions in testicular germ cells, where PRC1 depletion does not alter the proliferation of germ
274 cells (22). This may be due to the fact that PRC1 and PRC2 are not required for suppression of
275 *Cdkn2a* in germ cells (22, 45). The functional difference in testicular germ cells and Sertoli cells
276 highlights the context-dependent functions of Polycomb proteins. However, a recent study revealed
277 a novel activity by which PcGs can regulate cell proliferation through DNA replication
278 independently of *Cdkn2a* (46). Therefore, determining the detailed molecular mechanisms by
279 which PRC1 controls the proliferation of Sertoli cells will be important for future studies.
280
281 Another critical function of PRC1 in Sertoli cells is the suppression of the female gene
282 regulatory network. DMRT1 is a critical transcription factor that suppresses the expression of
283 female genes (5). While more than 10-fold upregulation of the female genes (*Rspo1* and *Foxl2*)
284 was observed for *Dmrt1* mutants (5), the degree of upregulation of these genes was modest in
285 PRC1RcKO Sertoli cells (Fig. 3). This finding, combined with genetic evidence, indicates that
286 DMRT1 could be the direct regulator of suppression of female genes, while PRC1-mediated
287 mechanisms could be a maintenance mechanism in response to the primary silencing mechanisms
288 determined by DMRT1. Another possibility is compensation by PRC1-independent suppression
289 mechanisms. While a portion of PRC2-mediated H3K27me3 is regulated by variant PRC1 (37, 38),
290 another portion of H3K27me3, mediated by canonical PRC1 and PRC2 complexes, is not
291 downstream of PRC1 (47). These PRC2-mediated mechanisms or other silencing machinery may
292 be responsible for the suppression of female genes.
293
294 The notion that Polycomb regulates the female gene regulatory network has been supported
295 by other recent evidence. In bipotential precursor cells, genes involved in sex determination are
296 marked with bivalent chromatin domains (14) that are prevalent in pluripotent stem cells and in
297 germ cells (48-53). Maintenance of the male fate was explained by the persistence of H3K27me3

298 on silent female genes in Sertoli cells (14). Consistent with PRC1's function found in the current
299 study, Polycomb-mediated silencing may globally suppress the female gene regulatory network.
300 We found that H2AK119ub was largely associated with this group of female genes (Fig. 5).
301 Therefore, it would be interesting to speculate that antagonistic male and female networks can be
302 directly coordinated by Polycomb protein functions, including the strong feedback mechanism
303 underlying both networks. These possibilities raise several outstanding questions to be addressed
304 in future studies. What are the functions of another Polycomb complex, PRC2, and of each
305 Polycomb complex component, including CBX2, in postnatal Sertoli cells? What is the function of
306 Polycomb in female granulosa cells, especially in the suppression of the male gene regulatory
307 network? Does Polycomb underlie the feedback regulation of each network to define sexual
308 identity? Our current study provides a foundation to explore these questions.
309
310 **Methods**
311
312 **Animals**
313 Generation of mutant *Ring1* and *Rnf2* floxed alleles were previously reported (54). *Amh-Cre*
314 transgenic mice were purchased from The Jackson Laboratory (Stock No: 007915) (20). *Rosa-Cre*
315 *ERT* mice were purchased from The Jackson Laboratory (Stock No: 008463) (55). A minimum of
316 three independent mice were analyzed for each experiment. Institutional Animal Care and Use
317 Committee approved this work: protocol no. IACUC2018-0040. Fertility tests were performed with
318 6-weeks old CD1 female mice (purchased from Charles river). At least 2 female mice were bred
319 with a male mouse for 2 weeks, and the fertility was evaluated by the ratio of pregnant to total
320 female mice and number of pups.
321
322
323 **Ligand test**
324 Blood samples were collected from C57BL/6N mice aged 8−11 weeks. Serum was separated
325 immediately and stored at -20°C. Hormone assays, including testosterone, estradiol, and follicle
326 stimulating hormone, were performed by the Center for Research in Reproduction at the University
327 of Virginia.
328
329 **Sertoli cell isolation**
330 Sertoli cells were isolated as previously described with minor modifications (56) and collected from
331 C57BL/6N mice aged 6–8 days. Testes were collected in a 24-well plate in Dulbecco's Modified

332 Eagle Medium (DMEM) supplemented with GlutaMax (Thermo Fisher Scientific), non-essential
333 amino acids (NEAA) (Thermo Fisher Scientific), and penicillin and streptomycin (Thermo Fisher
334 Scientific). After removing the *tunica albuginea* membrane, testes were digested with collagenase
335 (1 mg/ml) at 34°C for 20 min to remove interstitial cells, then centrifuged at 188×*g* for 5 min.
336 Tubules were washed with medium and then digested with trypsin (2.5 mg/ml) at 34°C for 20 min
337 to obtain a single-cell suspension. To remove KIT-positive spermatogonia, cells were washed with
338 magnetic cell-sorting (MACS) buffer (PBS supplemented with 0.5% BSA and 5 mM EDTA) and
339 incubated with CD117 (KIT) MicroBeads (Miltenyi Biotec) on ice for 20 min. Cells were separated
340 by autoMACS Pro Separator (Miltenyi Biotec) with the program "possel." Cells in the flow-
341 through fraction were washed with MACS buffer and incubated with CD90.2 (THY1) MicroBeads
342 (Miltenyi Biotec) on ice for 20 min to remove THY1-positive spermatogonia. Cells were separated
343 by autoMACS Pro Separator (Miltenyi Biotec) with the program "posseld." Cells in the flow-
344 through fraction were washed and plated in a 6-well plate for 1 h in the medium supplemented with
345 10% fetal bovine serum, which promotes adhesion of Sertoli cells. Purity was confirmed by
346 immunostaining.
347 For PRC1RcKO, cells were cultured for 4 days with 1 μM 4-OHT in Dulbecco's Modified
348 Eagle Medium (DMEM) supplemented with GlutaMax (Thermo Fisher Scientific), non-essential
349 amino acids (NEAA) (Thermo Fisher Scientific), and penicillin and streptomycin (Thermo Fisher
350 Scientific). The same medium was replaced 2 days after the initiation of the culture.
351
352 **Histological analysis and germ cell slide preparation**
353 For the preparation of testicular paraffin blocks, testes were fixed with 4% paraformaldehyde (PFA)
354 overnight at 4°C with gentle inverting. Testes were dehydrated and embedded in paraffin. For
355 histological analysis, 7 μm-thick paraffin sections were deparaffinized and stained with
356 hematoxylin and eosin. For immunofluorescence analysis of testicular sections, antigen retrieval
357 was performed by boiling the slides in target retrieval solution (DAKO) for 10 min and letting the
358 solution cool for 30 min. Sections were blocked with Blocking One Histo (Nacalai) for 1 h at room
359 temperature and then incubated with primary antibodies overnight at 4°C. The resulting signals
360 were detected by incubation with secondary antibodies conjugated to fluorophores (Thermo Fisher
361 Scientific). Sections were counterstained with DAPI. Images were obtained via a laser scanning
362 confocal microscope A1R (Nikon) and processed with NIS-Elements (Nikon) and ImageJ
363 (National Institutes of Health) (57).
364
365 **ChIP-sequencing, RNA-sequencing, and data analysis**

366 RNA-seq analyses were performed in the BioWardrobe Experiment Management System (58).
367 Briefly, reads were aligned by STAR (version STAR_2.5.3a)75 with default arguments except --
368 outFilterMultimapNmax 1 and --outFilterMismatchNmax 2. The --outFilterMultimapNmax
369 parameter was used to allow unique alignments only, and the --outFilterMismatchNmax parameter
370 was used to allow a maximum of 2 errors. NCBI RefSeq annotation from the mm10 UCSC genome
371 browser 76 was used, and canonical TSSs (1 TSS per gene) were analyzed. All reads from the
372 resulting .bam files were split for related isoforms with respect to RefSeq annotation. Then, the EM
373 algorithm was used to estimate the number of reads for each isoform. To detect differentially
374 expressed genes between two biological samples, a read count output file was input to the DESeq2
375 package (version 1.16.1); then, the program functions DESeqDataSetFromMatrix and DESeq were
376 used to compare each gene's expression level between two biological samples. Differentially
377 expressed genes were identified through binominal tests, thresholding Benjamini-Hochberg-
378 adjusted P values to <0.01. To perform gene ontology analyses, the functional annotation clustering
379 tool in DAVID (version 6.8) was used, and a background of all mouse genes was applied.
380 Biological process term groups with a significance of $P < 0.05$ (modified Fisher's exact test) were
381 considered significant.
382 Cross-linking ChIP-seq with the ChIPmetation method (59) was performed for
383 H2AK119ub, H3K27me3, and RNF2 as described previously (59). Data analysis for both ChIP-
384 seq and RNA-seq was performed in the BioWardrobe Experiment Management System
385 (https://github.com/Barski-lab/biowardrobe (58)). Briefly, reads were aligned to the mouse genome
386 (mm10) with Bowtie (version 1.0.0 (60)), assigned to RefSeq genes (which have one annotation
387 per gene) using the BioWardrobe algorithm, and displayed on a local mirror of the UCSC genome
388 browser as coverage. Peaks of H2AK119ub-, H3K27me3- and RNF2-enrichment were identified
389 using MACS2 (version 2.0.10.20130712 (61)). Pearson correlations for the genome-wide
390 enrichment of the peaks among ChIP-seq library replicates were analyzed using SeqMonk
391 (Babraham Institute). Average tag density profiles were calculated around gene bodies, including
392 5-kb upstream and 5-kb downstream of the genes. Resulting graphs were smoothed in 200-bp
393 windows. Enrichment levels for ChIP-seq experiments were calculated for 4-kb windows, promoter
394 regions of genes (±2 kb surrounding TSSs), and enhancer regions. To normalize tag value read
395 counts were multiplied by 1,000,000 and then divided by the total number of reads in each
396 nucleotide position. The total amount of tag values in promoter or enhancer regions were calculated
397 as enrichment. Microarray data was analyzed using the processed data (42). Differentially
398 expressed genes were identified through a p-value cutoff of 0.05, and a fold change cutoff of 2 for
399 the comparison between E13.5 XX supporting cells and E13.5 XY supporting cells. Highly

expressed genes in E13.5 XY supporting cells and in E13.5 XX supporting cells were termed as "Pre-sertoli genes" and "Pre-granulosa genes", respectively. RNA-seq and ChIP-seq data reported in this paper will be deposited to GEO.

Acknowledgments

We thank David Zarkower and Vivian Bardwell for their help and discussion in the initial phase of this project, Katie Gerhardt for editing the manuscript, and the members of the Namekawa and Maezawa laboratories for discussion and helpful comments regarding the manuscript. This work was supported by Grant-in-Aid for Research Activity Start-up (19K21196), the Takeda Science Foundation (2019), and the Uehara Memorial Foundation Research Incentive Grant (2018) to SM, NIH Grants GM119134 to AB, and GM098605 and GM122776 to SHN.

Figure legends

Figure 1. Deletion of PRC1 in Sertoli cells.

(**A**) RNF2 and RNF2-mediated H2AK119ub localized at GATA4-positive Sertoli cells (yellow arrows) in a testicular section at 6 weeks of age. Regions bordered by yellow squares are magnified in the right panels. Bars in the large panels: 50 μm. Bars in the magnified panels: 20 μm. (**B**) Genotypes and photographs of testes at 6 weeks of age. Measurement scale in the panel: 2 cm. (**C**) Testicular weight/body weight ratio ($\times 10^{-3}$) at 12 weeks of age. $P < 0.0001$, unpaired t-test. (**D, E**) Localization of H2AK119ub and GATA4 in PRC1ctrl and PRC1AcKO at embryonic day 15.5 (**D**) and 1 week of age (**E**). Regions bordered by yellow squares are magnified in the right panels. Bars in the large panels: 50 μm. Bars in the magnified panels: 20 μm. H2AK119ub$^-$ Sertoli cells in mutants are shown with white arrows. (**F**) The fertility of PRC1AcKO males, at 8-11 weeks of age and 5 months of age, were tested via crosses with CD1 wild-type females. Numbers of males tested are shown within the bars, and numbers of females with pups and all females are shown above the bars. $*P < 0.05$, Fisher's exact test. (**G**) Litter sizes of breeding tests at 8-11 weeks of age and 5 months of age. $*P < 0.05$, Welch's t-test. (**H**) Ligand hormone tests at 8-11 weeks of age testes. $*P < 0.05$, Welch's t-test. n.s., not significant.

Figure 2. PRC1 is required for proliferation of Sertoli cells.

(**A**) PCNA and Ki67 were not detected in GATA4-positive Sertoli cells (arrows) in a PRC1AcKO testicular section at 6 weeks of age, while PCNA and Ki67 were present in PRC1ctrl Sertoli cells. (**B**) Testicular sections of the indicated genotypes 1 day following the injection of EdU into males at 1 week of age. The presence of EdU-positive Sertoli cells (arrows) was decreased in PRC1AcKO

434 testes. Regions bordered by yellow squares are magnified in the right panels. Bars in the large
435 panels: 50 μm. Bars in the magnified panels: 20 μm.
436
437 **Figure 3. In Sertoli cells, PRC1 suppresses genes required for granulosa cells.**
438 (**A**) Genotypes and experiment schematic. Sertoli cells were isolated from P7 testes and cultured
439 for 4 days in the presence of 4-OHT prior to RNA-seq analyses. (**B**) The numbers of differentially
440 expressed genes detected by RNA-seq (≥1.5-fold change) in Sertoli cells (2 biological replicates)
441 between PRC1ctrl and PRC1RcKO. (**C**) Heatmaps showing gene expression patterns for
442 upregulated (left) and down-regulated (right) genes in Sertoli cells. (**D**) GO term analyses. (**E**)
443 Expression levels for representative Sertoli and granulosa genes. (**F, G**) H2AK119ub and
444 H3K27me3 ChIP-seq enrichment around the TSSs of representative Sertoli and granulosa genes.
445
446 **Figure 4. In Sertoli cells, Polycomb-mediated marks are enriched on genes required for**
447 **granulosa cells.**
448 (**A**) Genome track views of representative genes in the female gene regulatory network. ChIP-seq
449 enrichment in wild-type Sertoli cells is shown (top); RNA-seq peaks in PRC1ctrl and PRC1RcKO
450 Sertoli cells are shown (bottom). (**B**) Box-and-whisker plots showing distributions of enrichment
451 for ChIP-seq data. Central bars represent medians, the boxes encompass 50% of the data points,
452 and the whiskers indicate 90% of the data points. *P*, Mann-Whitney U tests. (**C**) Scatter plots
453 showing ChIP-seq enrichment (±2 kb around TSSs) of indicated modifications on genes
454 upregulated (left panels) and down-regulated (right panels) in Sertoli cells. The distribution of all
455 genes is shown with gray dots. (**D**) Average tag densities of H2AK119ub ChIP-seq enrichment.
456
457 **Figure 5. Polycomb inactivates the female gene regulatory network in Sertoli cells.**
458 (**A**) Box-and-whisker plots showing distributions of RNA-seq data. Central bars represent medians,
459 the boxes encompass 50% of the data points, and the whiskers indicate 90% of the data points. ***
460 $P < 0.0001$, Mann-Whitney U tests. (**B**) Scatter plots showing the Pearson correlation between
461 RNA-seq data for genes regulated in E13.5 support cells and P7 Sertoli cells. A linear trendline is
462 shown in blue. (**C**) Box-and-whisker plots showing distributions of enrichment for H2AK119ub
463 ChIP-seq data. Central bars represent medians, the boxes encompass 50% of the data points, and
464 the whiskers indicate 90% of the data points. *** $P < 0.0001$, ** $P < 0.005$, Mann-Whitney U tests.
465 (**D**) Scatter plots showing the Pearson correlation between ChIP-seq enrichment (±2 kb around
466 TSSs) and gene expression in Sertoli cells. A linear trendline is shown in blue.
467

468 **Figure S1. Deletion of PRC1 in Sertoli cells causes degeneration of testes at 6 weeks of age.**
469 Localization of H2AK119ub and GATA4 in PRC1ctrl and PRC1AcKO at 6 weeks of age. Regions
470 bordered by yellow squares are magnified in the right panels. Bars in the large panels: 50 μm. Bars
471 in the magnified panels: 20 μm. H2AK119ub$^-$ Sertoli cells in mutants are shown with white arrows.
472
473 **Figure S1. Biological replicates for RNA-seq and ChIP-seq data.**
474 (**A**) Scatter plots show the reproducibility of RNA-seq enrichment at individual peaks between
475 biological replicates. (**B**) Scatter plots show the reproducibility of and ChIP-seq enrichment at
476 individual peaks between biological replicates. Each peak was identified using MACS ($P < 1\times10^{-}$
477 ^{5}). H3K27ac ChIP-seq enrichment levels are shown in $\log_2$ RPKM values. The color scale indicates
478 RNA-seq or ChIP-seq peak density. Pearson correlation values (R) are shown.
479
480 **Figure S2. In Sertoli cells, H3K27me3 is enriched on genes required for granulosa cells.**
481 Average tag densities of H3K27me3 ChIP-seq enrichment on the groups of genes indicated in the
482 panel.
483
484 **Figure S3. Expression profiles of specifically expressed genes in E13.5 granulosa cells.**
485 Microarray analysis of gene expression in E13.5 supporting cells (42). Genes with the criteria of 2-
486 fold higher expression in E13.5 XX supporting cells and $P < 0.05$ were termed as "Pre-granulosa
487 genes" and shown in green. Genes with the criteria of 2-fold higher expression in E13.5 XY
488 supporting cells and $P < 0.05$ were termed as "Pre-sertoli genes" and shown in red.
489
490 **Figure S4. H3K27me3 is involved in the female gene regulatory network in Sertoli cells.** (**A**)
491 Box-and-whisker plots showing distributions of enrichment for H3K27me3 ChIP-seq data. Central
492 bars represent medians, the boxes encompass 50% of the data points, and the whiskers indicate
493 90% of the data points. *** $P < 0.0001$, Mann-Whitney U tests. (**B**) Scatter plots showing the
494 Pearson correlation between ChIP-seq enrichment (±2 kb around TSSs) and gene expression in
495 Sertoli cells. A linear trendline is shown in blue.
496
497
498

499 **References**

500 1. A. Swain, R. Lovell-Badge, Mammalian sex determination: a molecular drama. *Genes Dev*
501 **13**, 755-767 (1999).
502 2. D. Wilhelm, S. Palmer, P. Koopman, Sex determination and gonadal development in
503 mammals. *Physiol Rev* **87**, 1-28 (2007).
504 3. B. Capel, Vertebrate sex determination: evolutionary plasticity of a fundamental switch.
505 *Nature reviews. Genetics* **18**, 675-689 (2017).
506 4. T. Svingen, P. Koopman, Building the mammalian testis: origins, differentiation, and
507 assembly of the component cell populations. *Genes Dev* **27**, 2409-2426 (2013).
508 5. C. K. Matson *et al.*, DMRT1 prevents female reprogramming in the postnatal mammalian
509 testis. *Nature* **476**, 101-104 (2011).
510 6. C. K. Matson, D. Zarkower, Sex and the singular DM domain: insights into sexual
511 regulation, evolution and plasticity. *Nat Rev Genet* **13**, 163-174 (2012).
512 7. N. H. Uhlenhaut *et al.*, Somatic sex reprogramming of adult ovaries to testes by FOXL2
513 ablation. *Cell* **139**, 1130-1142 (2009).
514 8. A. Minkina *et al.*, DMRT1 protects male gonadal cells from retinoid-dependent sexual
515 transdifferentiation. *Dev Cell* **29**, 511-520 (2014).
516 9. R. E. Lindeman *et al.*, Sexual cell-fate reprogramming in the ovary by DMRT1. *Curr Biol*
517 **25**, 764-771 (2015).
518 10. L. Zhao, T. Svingen, E. T. Ng, P. Koopman, Female-to-male sex reversal in mice caused
519 by transgenic overexpression of Dmrt1. *Development (Cambridge, England)* **142**, 1083-
520 1088 (2015).
521 11. Y. Li *et al.*, beta-Catenin directs the transformation of testis Sertoli cells to ovarian
522 granulosa-like cells by inducing Foxl2 expression. *The Journal of biological chemistry*
523 **292**, 17577-17586 (2017).

524 12. B. Nicol *et al.*, Genome-wide identification of FOXL2 binding and characterization of
525 FOXL2 feminizing action in the fetal gonads. *Hum Mol Genet* **27**, 4273-4287 (2018).
526 13. Y. Katoh-Fukui *et al.*, Male-to-female sex reversal in M33 mutant mice. *Nature* **393**, 688-
527 692 (1998).
528 14. S. A. Garcia-Moreno *et al.*, CBX2 is required to stabilize the testis pathway by repressing
529 Wnt signaling. *PLoS genetics* **15**, e1007895 (2019).
530 15. S. Kuroki *et al.*, Epigenetic regulation of mouse sex determination by the histone
531 demethylase Jmjd1a. *Science* **341**, 1106-1109 (2013).
532 16. L. Ringrose, R. Paro, Polycomb/Trithorax response elements and epigenetic memory of
533 cell identity. *Development (Cambridge, England)* **134**, 223-232 (2007).
534 17. L. Aloia, B. Di Stefano, L. Di Croce, Polycomb complexes in stem cells and embryonic
535 development. *Development (Cambridge, England)* **140**, 2525-2534 (2013).
536 18. J. A. Simon, R. E. Kingston, Occupying chromatin: Polycomb mechanisms for getting to
537 genomic targets, stopping transcriptional traffic, and staying put. *Molecular cell* **49**, 808-
538 824 (2013).
539 19. M. Endoh *et al.*, Histone H2A mono-ubiquitination is a crucial step to mediate PRC1-
540 dependent repression of developmental genes to maintain ES cell identity. *PLoS genetics*
541 **8**, e1002774 (2012).
542 20. R. W. Holdcraft, R. E. Braun, Androgen receptor function is required in Sertoli cells for
543 the terminal differentiation of haploid spermatids. *Development (Cambridge, England)*
544 **131**, 459-467 (2004).
545 21. M. del Mar Lorente *et al.*, Loss- and gain-of-function mutations show a polycomb group
546 function for Ring1A in mice. *Development (Cambridge, England)* **127**, 5093-5100 (2000).
547 22. S. Maezawa *et al.*, Polycomb directs timely activation of germline genes in
548 spermatogenesis. *Genes & development* **31**, 1693-1703 (2017).

549 23. S. Yokobayashi *et al.*, PRC1 coordinates timing of sexual differentiation of female
550 primordial germ cells. *Nature* **495**, 236-240 (2013).
551 24. E. Posfai *et al.*, Polycomb function during oogenesis is required for mouse embryonic
552 development. *Genes & development* **26**, 920-932 (2012).
553 25. Z. Gao *et al.*, PCGF homologs, CBX proteins, and RYBP define functionally distinct PRC1
554 family complexes. *Molecular cell* **45**, 344-356 (2012).
555 26. O. O. Oduwole, H. Peltoketo, I. T. Huhtaniemi, Role of Follicle-Stimulating Hormone in
556 Spermatogenesis. *Front Endocrinol (Lausanne)* **9**, 763 (2018).
557 27. R. M. Sharpe, C. McKinnell, C. Kivlin, J. S. Fisher, Proliferation and functional maturation
558 of Sertoli cells, and their relevance to disorders of testis function in adulthood.
559 *Reproduction (Cambridge, England)* **125**, 769-784 (2003).
560 28. S. Vainio, M. Heikkila, A. Kispert, N. Chin, A. P. McMahon, Female development in
561 mammals is regulated by Wnt-4 signalling. *Nature* **397**, 405-409 (1999).
562 29. A. A. Chassot *et al.*, Activation of beta-catenin signaling by Rspo1 controls differentiation
563 of the mammalian ovary. *Hum Mol Genet* **17**, 1264-1277 (2008).
564 30. D. Schmidt *et al.*, The murine winged-helix transcription factor Foxl2 is required for
565 granulosa cell differentiation and ovary maintenance. *Development (Cambridge, England)*
566 **131**, 933-942 (2004).
567 31. P. Parma *et al.*, R-spondin1 is essential in sex determination, skin differentiation and
568 malignancy. *Nature genetics* **38**, 1304-1309 (2006).
569 32. C. Ottolenghi *et al.*, Loss of Wnt4 and Foxl2 leads to female-to-male sex reversal extending
570 to germ cells. *Human molecular genetics* **16**, 2795-2804 (2007).
571 33. V. P. Vidal, M. C. Chaboissier, D. G. de Rooij, A. Schedl, Sox9 induces testis development
572 in XX transgenic mice. *Nature genetics* **28**, 216-217 (2001).
573 34. C. S. Raymond *et al.*, Evidence for evolutionary conservation of sex-determining genes.
574 *Nature* **391**, 691-695 (1998).

575 35. C. S. Raymond, M. W. Murphy, M. G. O'Sullivan, V. J. Bardwell, D. Zarkower, Dmrt1, a
576 gene related to worm and fly sexual regulators, is required for mammalian testis
577 differentiation. *Genes & development* **14**, 2587-2595 (2000).
578 36. H. H. Yao, W. Whoriskey, B. Capel, Desert Hedgehog/Patched 1 signaling specifies fetal
579 Leydig cell fate in testis organogenesis. *Genes & development* **16**, 1433-1440 (2002).
580 37. N. P. Blackledge *et al.*, Variant PRC1 complex-dependent H2A ubiquitylation drives PRC2
581 recruitment and polycomb domain formation. *Cell* **157**, 1445-1459 (2014).
582 38. S. Cooper *et al.*, Targeting polycomb to pericentric heterochromatin in embryonic stem
583 cells reveals a role for H2AK119u1 in PRC2 recruitment. *Cell reports* **7**, 1456-1470 (2014).
584 39. U. Jochumsen *et al.*, Mutation analysis of FOXF2 in patients with disorders of sex
585 development (DSD) in combination with cleft palate. *Sex Dev* **2**, 302-308 (2008).
586 40. H. Du, H. S. Taylor, The Role of Hox Genes in Female Reproductive Tract Development,
587 Adult Function, and Fertility. *Cold Spring Harb Perspect Med* **6**, a023002 (2015).
588 41. T. I. Lee *et al.*, Control of developmental regulators by Polycomb in human embryonic
589 stem cells. *Cell* **125**, 301-313 (2006).
590 42. S. A. Jameson *et al.*, Temporal transcriptional profiling of somatic and germ cells reveals
591 biased lineage priming of sexual fate in the fetal mouse gonad. *PLoS genetics* **8**, e1002575
592 (2012).
593 43. J. J. Jacobs, K. Kieboom, S. Marino, R. A. DePinho, M. van Lohuizen, The oncogene and
594 Polycomb-group gene bmi-1 regulates cell proliferation and senescence through the ink4a
595 locus. *Nature* **397**, 164-168 (1999).
596 44. M. Serrano *et al.*, Role of the INK4a locus in tumor suppression and cell mortality. *Cell*
597 **85**, 27-37 (1996).
598 45. W. Mu, J. Starmer, A. M. Fedoriw, D. Yee, T. Magnuson, Repression of the soma-specific
599 transcriptome by Polycomb-repressive complex 2 promotes male germ cell development.
600 *Genes & development* **28**, 2056-2069 (2014).

601 46. A. Piunti *et al.*, Polycomb proteins control proliferation and transformation independently
602 of cell cycle checkpoints by regulating DNA replication. *Nature communications* **5**, 3649
603 (2014).
604 47. A. Laugesen, J. W. Hojfeldt, K. Helin, Molecular Mechanisms Directing PRC2
605 Recruitment and H3K27 Methylation. *Mol Cell* **74**, 8-18 (2019).
606 48. B. E. Bernstein *et al.*, A bivalent chromatin structure marks key developmental genes in
607 embryonic stem cells. *Cell* **125**, 315-326 (2006).
608 49. S. S. Hammoud *et al.*, Distinctive chromatin in human sperm packages genes for embryo
609 development. *Nature* **460**, 473-478 (2009).
610 50. B. J. Lesch, G. A. Dokshin, R. A. Young, J. R. McCarrey, D. C. Page, A set of genes critical
611 to development is epigenetically poised in mouse germ cells from fetal stages through
612 completion of meiosis. *Proceedings of the National Academy of Sciences of the United*
613 *States of America* **110**, 16061-16066 (2013).
614 51. H. S. Sin, A. V. Kartashov, K. Hasegawa, A. Barski, S. H. Namekawa, Poised chromatin
615 and bivalent domains facilitate the mitosis-to-meiosis transition in the male germline. *BMC*
616 *biology* **13**, 53 (2015).
617 52. S. Maezawa *et al.*, Polycomb protein SCML2 facilitates H3K27me3 to establish bivalent
618 domains in the male germline. *Proceedings of the National Academy of Sciences of the*
619 *United States of America* **115**, 4957-4962 (2018).
620 53. S. Maezawa, M. Yukawa, K. G. Alavattam, A. Barski, S. H. Namekawa, Dynamic
621 reorganization of open chromatin underlies diverse transcriptomes during spermatogenesis.
622 *Nucleic Acids Res* **46**, 593-608 (2018).
623 54. C. Cales *et al.*, Inactivation of the polycomb group protein Ring1B unveils an
624 antiproliferative role in hematopoietic cell expansion and cooperation with tumorigenesis
625 associated with Ink4a deletion. *Mol Cell Biol* **28**, 1018-1028 (2008).

626 55. A. Ventura *et al.*, Restoration of p53 function leads to tumour regression in vivo. *Nature*
627 **445**, 661-665 (2007).
628 56. Y. F. Chang, J. S. Lee-Chang, S. Panneerdoss, J. A. MacLean, 2nd, M. K. Rao, Isolation of
629 Sertoli, Leydig, and spermatogenic cells from the mouse testis. *Biotechniques* **51**, 341-342,
630 344 (2011).
631 57. C. A. Schneider, W. S. Rasband, K. W. Eliceiri, NIH Image to ImageJ: 25 years of image
632 analysis. *Nat Methods* **9**, 671-675 (2012).
633 58. A. V. Kartashov, A. Barski, BioWardrobe: an integrated platform for analysis of
634 epigenomics and transcriptomics data. *Genome biology* **16**, 158 (2015).
635 59. C. Schmidl, A. F. Rendeiro, N. C. Sheffield, C. Bock, ChIPmentation: fast, robust, low-
636 input ChIP-seq for histones and transcription factors. *Nat Methods* **12**, 963-965 (2015).
637 60. B. Langmead, C. Trapnell, M. Pop, S. L. Salzberg, Ultrafast and memory-efficient
638 alignment of short DNA sequences to the human genome. *Genome biology* **10**, R25 (2009).
639 61. Y. Zhang *et al.*, Model-based analysis of ChIP-Seq (MACS). *Genome biology* **9**, R137
640 (2008).
641

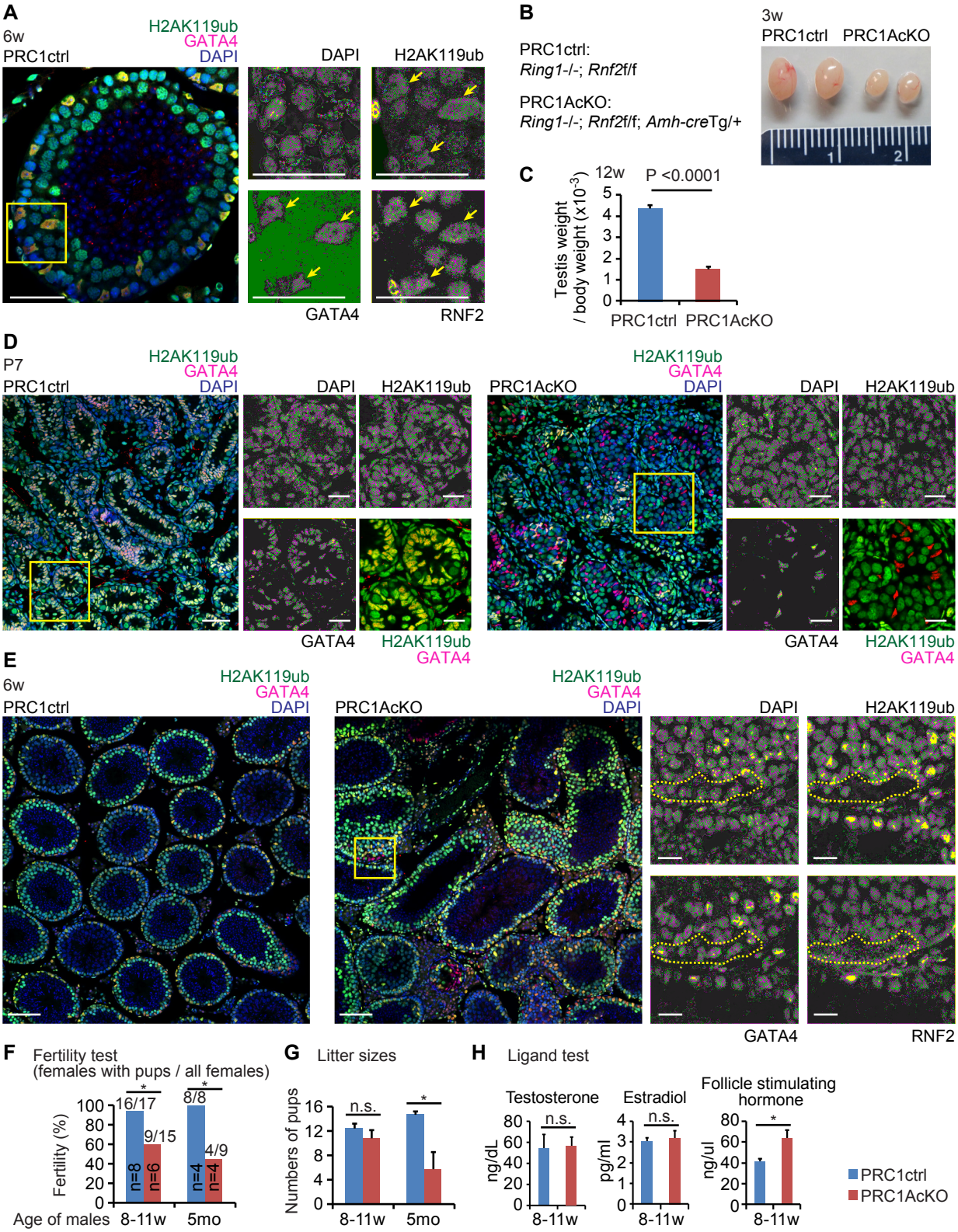
A
6w
PRC1ctrl
H2AK119ub
GATA4
DAPI
DAPI
H2AK119ub
GATA4
RNF2
B
PRC1ctrl:
Ring1-/-; Rnf2f/f
PRC1AcKO:
Ring1-/-; Rnf2f/f; Amh-creTg/+
3w
PRC1ctrl
PRC1AcKO
C
12w
P <0.0001
Testis weight / body weight (x10-3)
PRC1ctrl
PRC1AcKO
D
P7
PRC1ctrl
PRC1AcKO
H2AK119ub
GATA4
DAPI
GATA4
E
6w
PRC1ctrl
PRC1AcKO
GATA4
RNF2
F
Fertility test
(females with pups / all females)
Fertility (%)
16/17
9/15
8/8
4/9
n=8
n=6
n=4
n=4
Age of males
8-11w
5mo
G
Litter sizes
Numbers of pups
n.s.
8-11w
5mo
H
Ligand test
Testosterone
Estradiol
Follicle stimulating hormone
ng/dL
pg/ml
ng/ul
n.s.
PRC1ctrl
PRC1AcKO

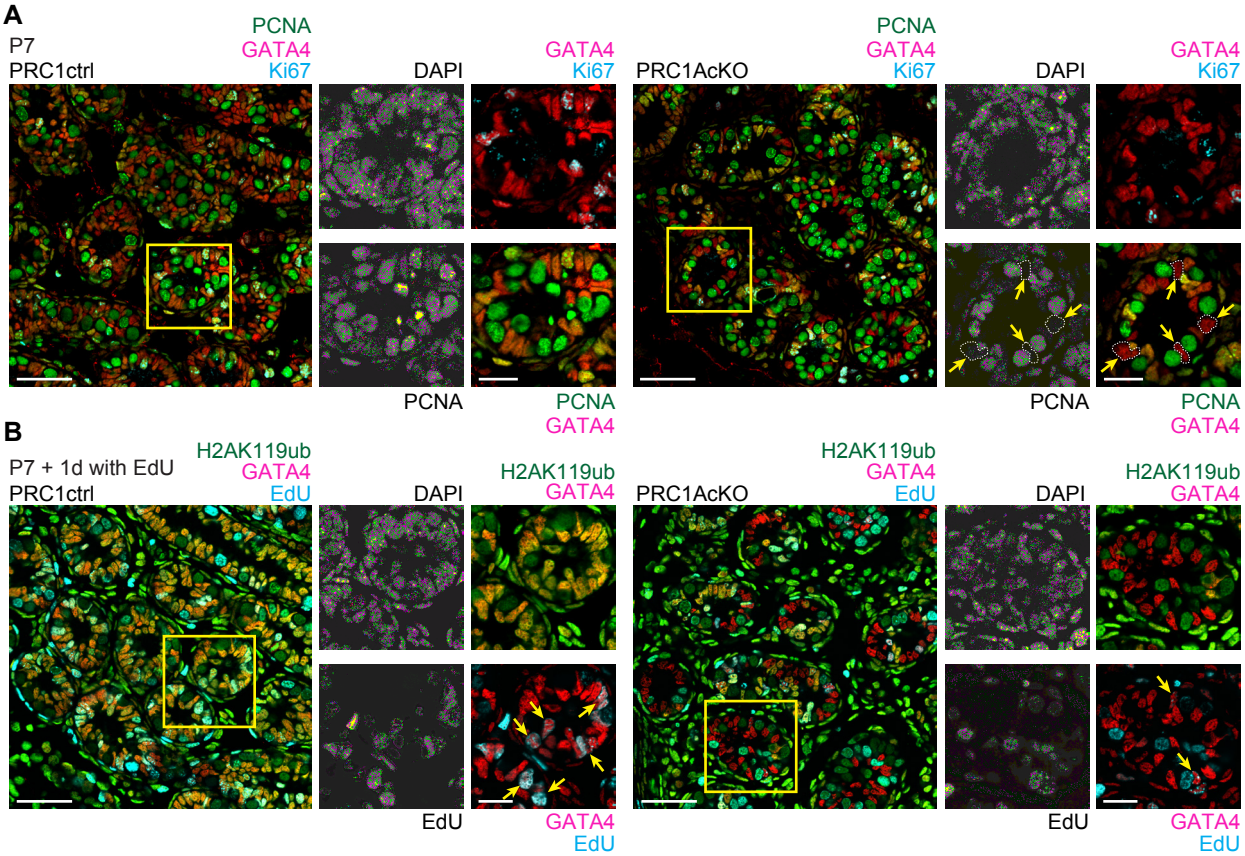
A
P7
PRC1ctrl
PCNA
GATA4
Ki67
DAPI
GATA4
Ki67
PCNA
PCNA
GATA4
PRC1AcKO
PCNA
GATA4
Ki67
DAPI
GATA4
Ki67
PCNA
PCNA
GATA4
B
P7 + 1d with EdU
PRC1ctrl
H2AK119ub
GATA4
EdU
DAPI
H2AK119ub
GATA4
EdU
GATA4
EdU
PRC1AcKO
H2AK119ub
GATA4
EdU
DAPI
H2AK119ub
GATA4
EdU
GATA4
EdU

Maezawa_Fig3

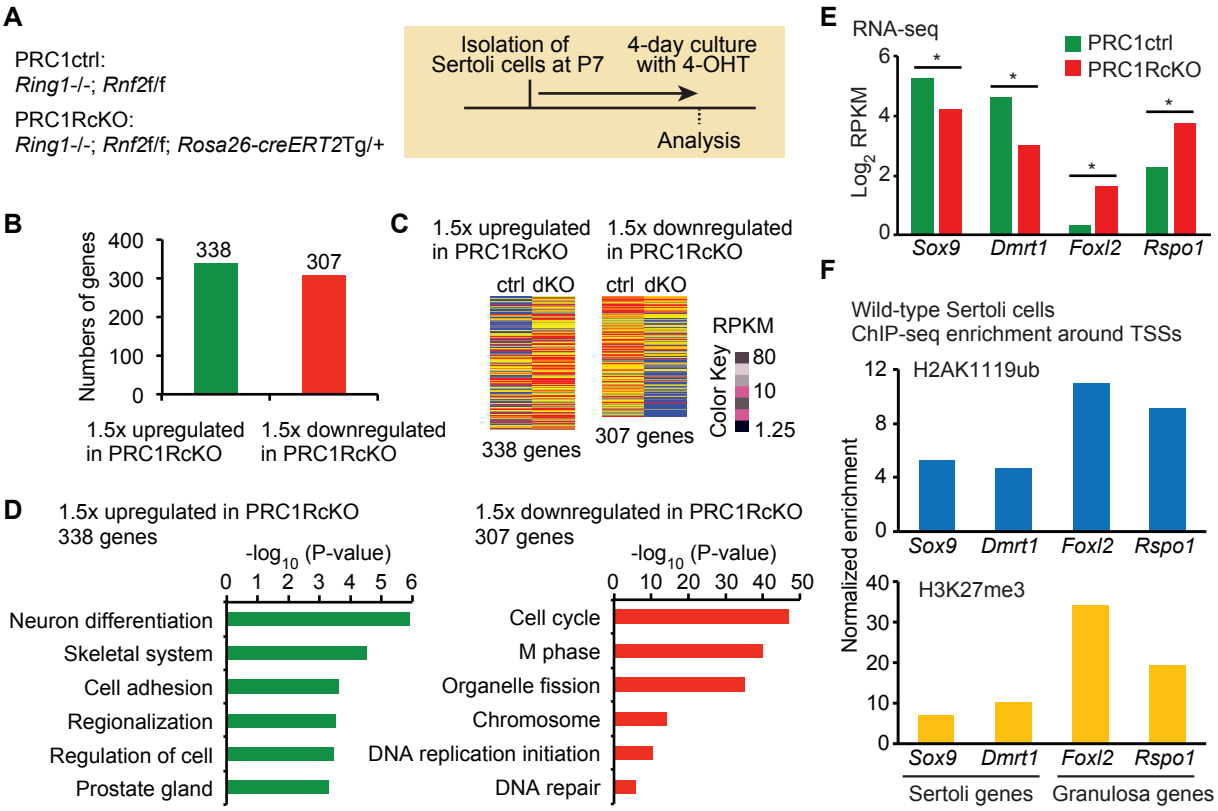

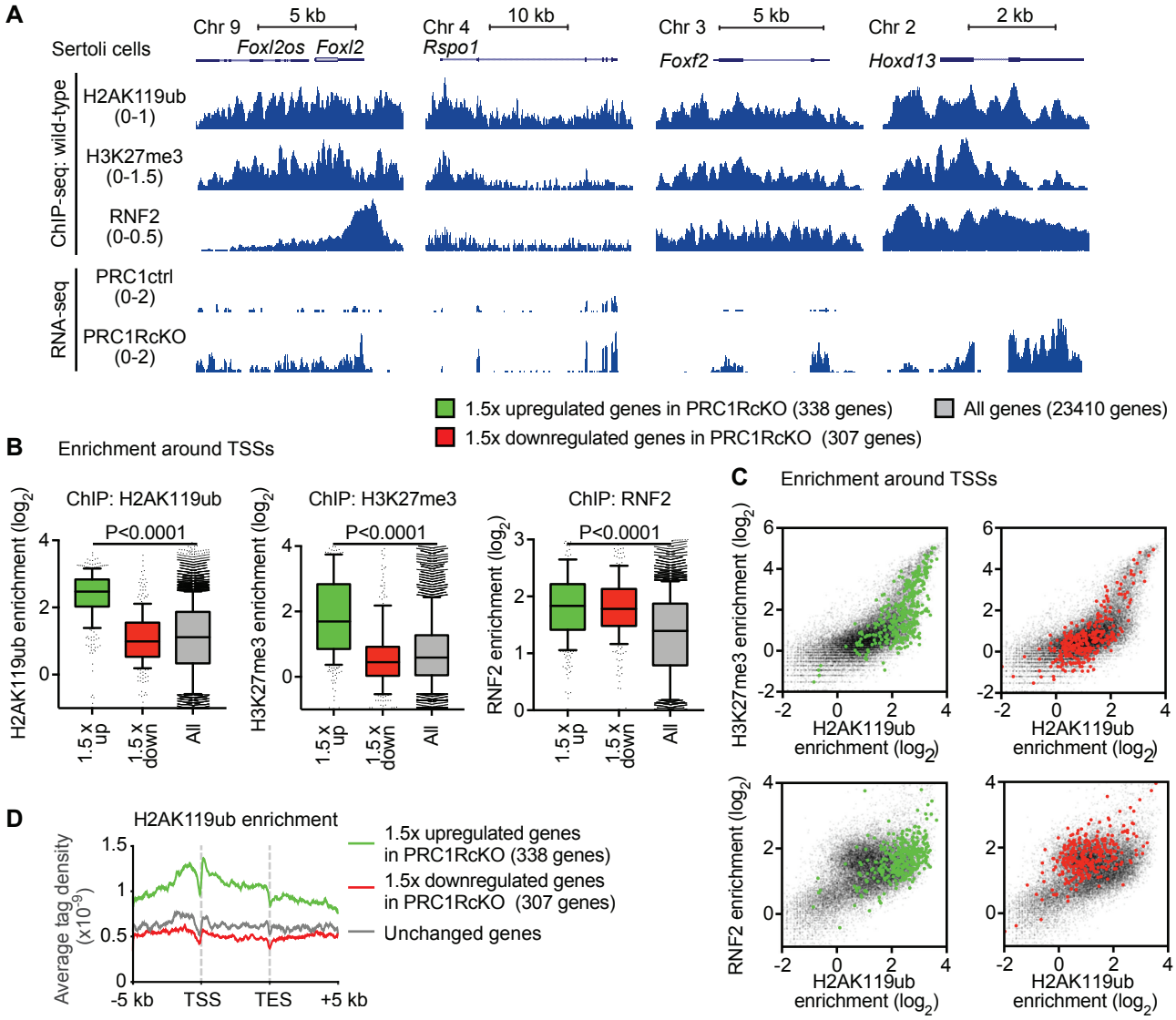
A
Sertoli cells
Chr 9
5 kb
Foxl2os
Foxl2
Chr 4
10 kb
Rspo1
Chr 3
5 kb
Foxf2
Chr 2
2 kb
Hoxd13
ChIP-seq: wild-type
H2AK119ub (0-1)
H3K27me3 (0-1.5)
RNF2 (0-0.5)
RNA-seq
PRC1ctrl (0-2)
PRC1RcKO (0-2)
1.5x upregulated genes in PRC1RcKO (338 genes)
1.5x downregulated genes in PRC1RcKO (307 genes)
All genes (23410 genes)
B
Enrichment around TSSs
ChIP: H2AK119ub
ChIP: H3K27me3
ChIP: RNF2
P<0.0001
H2AK119ub enrichment (log2)
H3K27me3 enrichment (log2)
RNF2 enrichment (log2)
1.5 x up
1.5 x down
All
C
Enrichment around TSSs
H3K27me3 enrichment (log2)
RNF2 enrichment (log2)
H2AK119ub enrichment (log2)
D
H2AK119ub enrichment
Average tag density (x10-9)
-5 kb
TSS
TES
+5 kb
1.5x upregulated genes in PRC1RcKO (338 genes)
1.5x downregulated genes in PRC1RcKO (307 genes)
Unchanged genes

Maezawa_Fig5

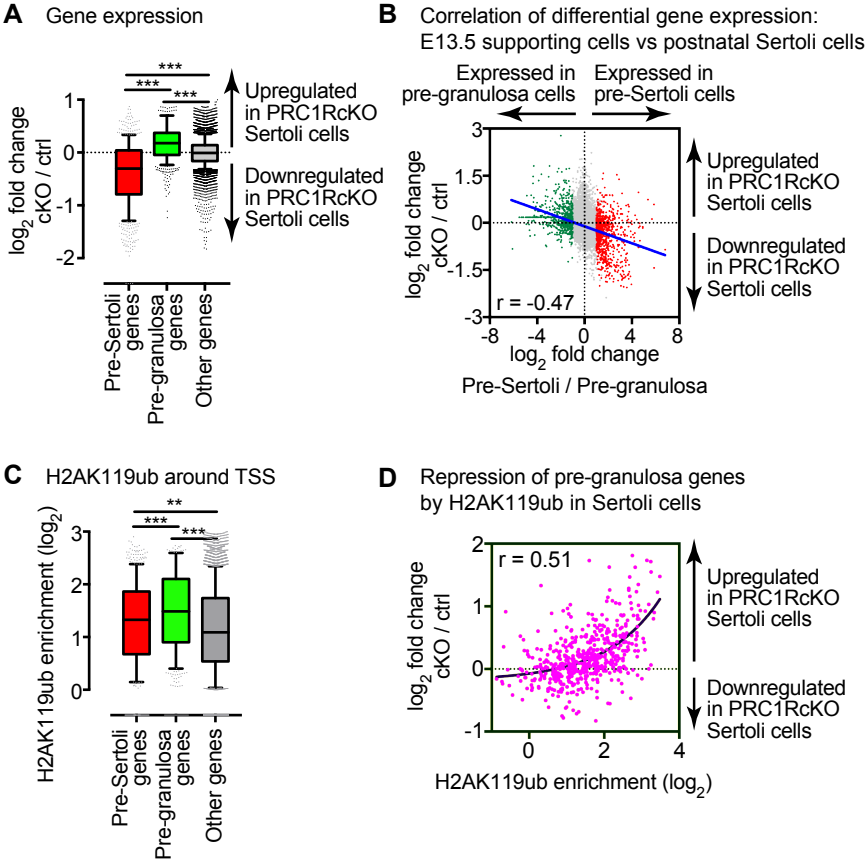

Maezawa_Fig. S1

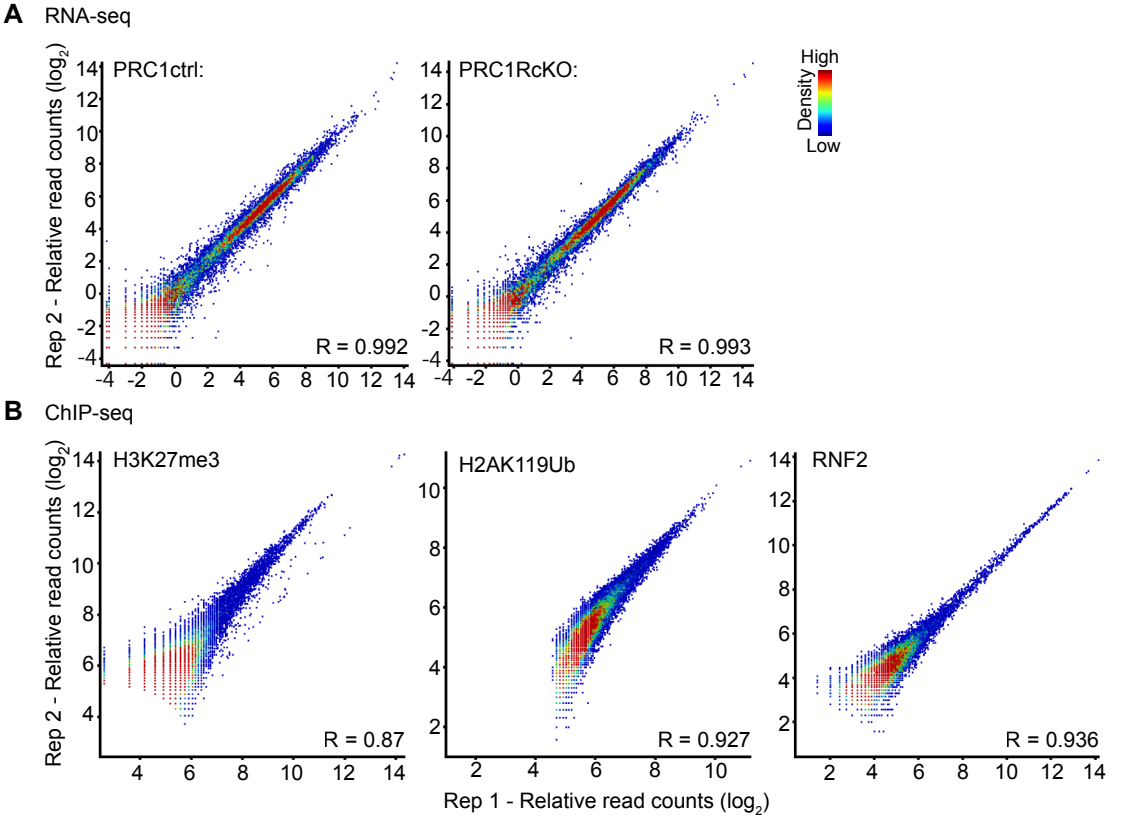

Maezawa_Fig. S2

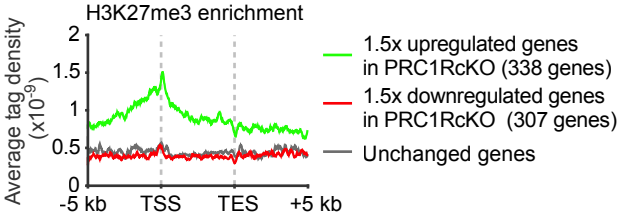

Maezawa_Fig. S3

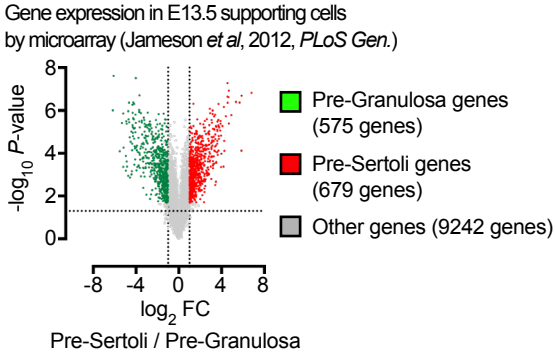
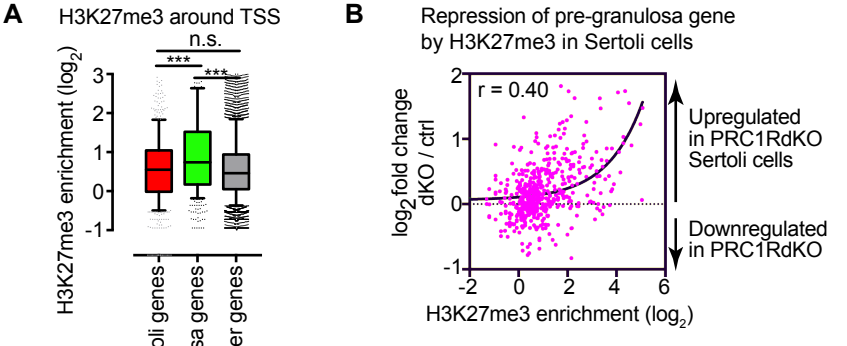
Maezawa_Fig. S4